# Efficient sum-of-exponentials approximations for the heat kernel and their applications

Shidong Jiang [*]     Leslie Greengard [†]     Shaobo Wang [‡]

September 13, 2018

## Abstract

In this paper, we show that efficient separated sum-of-exponentials approximations can be constructed for the heat kernel in any dimension. In one space dimension, the heat kernel admits an approximation involving a number of terms that is of the order $O(\log(\frac{T}{\delta})(\log(\frac{1}{\epsilon}) + \log\log(\frac{T}{\delta})))$ for any $x \in \mathbb{R}$ and $\delta \leq t \leq T$, where $\epsilon$ is the desired precision. In all higher dimensions, the corresponding heat kernel admits an approximation involving only $O(\log^2(\frac{T}{\delta}))$ terms for fixed accuracy $\epsilon$. These approximations can be used to accelerate integral equation-based methods for boundary value problems governed by the heat equation in complex geometry. The resulting algorithms are nearly optimal. For $N_S$ points in the spatial discretization and $N_T$ time steps, the cost is $O(N_S N_T \log^2 \frac{T}{\delta})$ in terms of both memory and CPU time for fixed accuracy $\epsilon$. The algorithms can be parallelized in a straightforward manner. Several numerical examples are presented to illustrate the accuracy and stability of these approximations.

## 1   Introduction

Our study of the heat kernel and its approximation is motivated by an interest in developing efficient methods for the solution of the heat equation

$$U_t = \Delta U, \quad U(x,0) = U_0(x), \tag{1}$$

subject, for example, to Dirichlet boundary conditions

$$U(x,t) = f(x,t)\big|_{\Gamma(t)} \tag{2}$$

---

[*]Department of Mathematical Sciences, New Jersey Institute of Technology, Newark, New Jersey 07102. *email*: shidong.jiang@njit.edu Thw work of this author was supported in part by NSF under grant CCF-0905395.

[†]Courant Institute of Mathematical Sciences, New York University, New York, NY 10012. *email*: greengard@courant.nyu.edu The work of this author was supported in part by the U.S. Department of Energy under contract DEFGO288ER25053.

[‡]Department of Mathematical Sciences, New Jersey Institute of Technology, Newark, New Jersey 07102. *email*: sw228@njit.edu

in a *moving* space-time domain $\Omega_T = \prod_{t=0}^{T} \Omega(t)$, where $\Gamma(t)$ is the boundary of $\Omega(t)$. More precisely, we are interested in accelerating methods based on heat potentials [16, 40], which seek to represent $U$ in terms of a single or double layer potential,

$$S(\sigma)(x,t) = \int_0^t \int_{\Gamma(t)} \frac{\partial}{\partial n_y} G(x-y, t-\tau)\sigma(y,\tau)ds_y d\tau \tag{3}$$

and

$$D(\sigma)(x,t) = \int_0^t \int_{\Gamma(t)} \frac{\partial}{\partial n_y} G(x-y, t-\tau)\sigma(y,\tau)ds_y d\tau \,, \tag{4}$$

respectively, where $G(x,t)$ is the heat kernel

$$G(x,t) = \frac{1}{(4\pi t)^{d/2}} e^{-\frac{|x|^2}{4t}} \,,$$

$n_y$ denotes the unit outward normal to $\Gamma(\tau)$ at the point $y = y(\tau)$, and $\sigma$ is an unknown surface density.

For the Dirichlet problem (1), it is standard to represent $U$ using the double layer heat potential:

$$U(x,t) = D(\sigma)(x,t) + V(x,t) \tag{5}$$

where $V(x,t)$ denotes the *initial potential*

$$V(x,t) = \int_{\Omega(0)} G(x-y, t)U_0(y)ds_y \,.$$

Imposing the boundary condition and using standard jump relations [16, 40] leads to the Volterra integral equation of the second kind

$$-\frac{1}{2}\sigma(x,t) + D^*(\sigma)(x,t) = f(x,t) - V(x,t) \tag{6}$$

on the space-time boundary $\Gamma_T = \prod_{t=0}^{T} \Gamma(t)$. Here, $D^*(\sigma)(x,t)$ denotes the principal value of the double layer potential.

It is convenient both analytically and numerically to decompose the double layer potential into two pieces: a *history* part $D_H$ and a *local* part $D_L$. Letting $\delta$ be a small positive parameter, we write

$$D(\sigma)(x,t) = D_H(\sigma)(x,t,\delta) + D_L(\sigma)(x,t,\delta),$$

where

$$D_H(\sigma)(x,t,\delta) = \int_0^{t-\delta} \int_{\Gamma(t)} \frac{\partial}{\partial n_y} G(x-y, t-\tau)\sigma(y,\tau)ds_y d\tau \tag{7}$$

2

and

$$D_L(\sigma)(x,t,\delta) = \int_{t-\delta}^{t} \int_{\Gamma(t)} \frac{\partial}{\partial n_y} G(x-y,t-\tau)\sigma(y,\tau)ds_y d\tau \,. \tag{8}$$

A major advantage of the integral equation formulation is that high order accuracy can be achieved through the use of suitable quadratures, even when the boundary is in motion (see, for example, [31]). A second advantage is that the equation (6) can be written in the form

$$-\frac{1}{2}\sigma(x,t) + D_L^*(\sigma)(x,t) = f(x,t) - V(x,t) - D_H^*(\sigma)(x,t) \tag{9}$$

Since the history part is already known and the norm of $D_L$ can be shown to be of the order $\|D_L\| = O(\sqrt{\delta})$ [20], the equation (9) can be solved by $2k$ steps of fixed point iteration to an accuracy of $\delta^k$.

There is a substantial engineering literature on boundary integral eqautions for heat flow (see, for example, [10, 36]). In the mathematical literature, it is worth noting the work of McIntyre [38], Noon [39], Chapko and Kress [13], and the survey article of Costabel [15].

The major disadvantage of numerical methods based on heat potentials, however, is their history-dependence. Simply evaluating $D\sigma$ at a sequence of time steps $t_n = n\Delta t$, for $n = 0, \ldots, N_T$, clearly requires an amount of work of the order $O(N_T^2 N_S^2)$, where $N_S$ denotes the number of points in the discretization of the boundary. While direct discretization methods have been used for (9), in the absence of fast algorithms it is difficult to argue that integral equation methods would be methods of choice for large-scale simulation. In the last two decades, however, a variety of schemes have been developed to overcome this obstacle. The scheme of [19] used discrete Fourier methods to represent the history part, while [9] replaced the Fourier representation with a regular (physical space) grid on which to update $D_H$. In [18], the problem of exterior heat flow was considered using the continuous Fourier transform in the spatial variables. Sethian and Strain [42] and Ibanez and Power [24] developed variants of the fast algorithm of [19] in the analysis of solidification, melting and crystal growth. More recently, Tausch [45] developed an interesting space-time "fast-multipole-like" method that also overcomes the cost of history-dependence (although it involves a hierarchical decomposition of the entire space-time domain).

A somewhat different approach to overcoming history dependence is based on using the Laplace transform in the time variable, leading to what are sometimes called "Laplace transform boundary element methods" [15, 22, 34, 41]. That is the approach we consider here, for the following reasons:

1. The Fourier methods of [18, 19] assume that the spatial domain of interest is finite (even when considering exterior problems). Both the computation of the Fourier modes and the evaluation of the solution at large distances can involve highly oscillatory integrals.

2. The required number of Fourier modes in [18, 19] is $O\left(\left(\frac{a}{\sqrt{\delta}}\right)^d\right)$, where $a$ is a bound on the extent of the domain in each spatial direction. This makes the method inefficient for small $\delta$.

Using the Laplace transform avoids both of these difficulties and leads to a sum-of-exponentials approximation of the heat kernel that is asymptotically optimal (although in the end, hybrid schemes may yield better constants).

Sum-of-exponentials approximations of convolution kernels have many applications in scientific computing. They permit, for example, the construction of diagonal forms for translation operators. We refer the reader to [14, 49] for their use in the elliptic case in accelerating fast multipole methods. They also permit the development of highly efficient nonreflecting boundary conditions for the wave and the Schrödinger equations [2, 3, 22, 25, 26, 35].

Function approximation using sums of exponentials is a highly nonlinear problem, so that the numerical construction of such approximations is nontrivial. In a series of papers, Beylkin and Monzón [4, 5, 6] carried out a detailed investigation and developed efficient and robust algorithms when given function values on a fixed interval. In some cases, the function of interest can be represented as a parametrized integral with exponential functions in the integrand, in which case generalized Gaussian quadrature methods [11, 37] can also be used. In other cases, however, the function being approximated, say $f(t)$ is only accessible as the inverse Laplace transform of an explicitly computable function, say $\hat{f}(s)$. If $\hat{f}(s)$ is sectorial (i.e., holomorphic on the complement of some acute sector containing the negative real axis for $s \in \mathbb{C}$), then the truncated trapezoidal or midpoint rule can be used in conjunction with carefully chosen contour integrals, leading to efficient and accurate sum-of-exponentials approximations. López-Fernández, Palencia, and Schädle, for example, have made effective use of various hyperbolic contours [32, 33]. On the other hand, if the Laplace transform $\hat{f}(s)$ does not have such well-defined properties, one may instead try to find a sum-of-poles approximation in the $s$-domain, from which a sum-of-exponentials approximation for $f(t)$ can be obtained by inverting the sum-of-poles approximation analytically (see, for example, [48]).

In this paper, we construct efficient *separated* sum-of-exponentials approximations for the free-space heat kernel. In particular, We show that the one-dimensional heat kernel $\frac{1}{\sqrt{4\pi t}}e^{-|x|^2/(4t)}$ admits an approximation of the form

$$\frac{1}{\sqrt{4\pi t}}e^{-|x|^2/(4t)} \approx \sum_{i=1}^{N_1} w_i e^{-s_i t} e^{\sqrt{s_i}|x|}$$

for any $t \in [\delta, T]$ and $x \in \mathbb{R}$, where $N_1 = O(\log(\frac{T}{\delta})(\log(\frac{1}{\epsilon}) + \log\log(\frac{T}{\delta})))$ where $\epsilon$ is the desired precision. In the $d$-dimensional case ($d > 1$), the heat kernel $\frac{1}{(4\pi t)^{d/2}}e^{-|x|^2/(4t)}$ admits an approximation of the form

$$\frac{1}{(4\pi t)^{d/2}}e^{-|x|^2/(4t)} \approx \sum_{j=1}^{N_2} \tilde{w}_j e^{-\lambda_j t} \sum_{i=1}^{N_1} w_i e^{-s_i t} e^{\sqrt{s_i}|x|} \tag{10}$$

for all $t \in [\delta, T]$ and $x \in \mathbb{R}^d$, where $N_1 = O(\log(\frac{T}{\delta})(\log(\frac{1}{\epsilon}) + \log\log(\frac{T}{\delta})))$ and $N_2 = O\left(\log\left(\frac{1}{\epsilon}\right) \cdot \left(\log\frac{T}{\delta} + \log\frac{1}{\epsilon}\right)\right)$. Both our construction and proof draw on earlier work, especially [6, 33].

The paper is organized as follows. In Section 2, we collect some useful results mainly from [6, 33]. After developing the sum-of-exponentials representations in Section 3, we then discuss their application to boundary value problems governed by the heat equation in Section 4. The basic idea is to use the sum-of-exponentials approximation for the computation of the history part (such as $D_H(\sigma)$ above), since the parameter $\delta$ separates the time integration variable $\tau$ from the current time $t$ so that $t - \tau \in [\delta, T]$. Since the temporal dependence for each term in (10) involves a simple exponential, the convolution in time can be easily computed using standard recurrence relations, as in [18, 19]. Furthermore, the convolutions in space can be evaluated by a variety of fast algorithms, such as variants of the fast multipole method. These issues are discussed in section 4. With $\delta = \Delta t$, where $\Delta t$ is a fixed time step, the total computational cost for evaluating $D_H(\sigma)$ is easily seen to be of the order $O\left(N_S N_T \log(N_S)\log^2(N_T)\right)$, and the memory requirements are of the order $O\left(N_S \log^2(N_T)\right)$ for fixed accuracy $\epsilon$.

# 2 Analytical preliminaries

In this section, we collect some results from [6, 33] which will be used in subsequent sections.

The following lemma provides an error estimate for the sum-of-exponentials approximation obtained by the truncated trapezoidal rule discretization of a certain contour integral in the Laplace domain.

**Lemma 1.** [Adapted from [33].] *Suppose that $U(z)$ is holomorphic on $W = \mathbb{C} \setminus (-\infty, 0]$ and satisfies the estimate*

$$\|U(z)\| \leq \frac{1}{2|z|^{1/2}} \tag{11}$$

*for $z \in W$. Suppose that $u(t) = \frac{1}{2\pi i}\int_\Gamma e^{tz}U(z)dz$ is the inverse Laplace transform of $U$. Suppose further that $\alpha$ and $\beta$ satisfy the condition $0 < \alpha - \beta < \alpha + \beta < \frac{\pi}{2}$, $0 < \theta < 1$, and that $\Gamma$ is chosen to be the left branch of the hyperbola*

$$\Gamma = \{\lambda T(x) : x \in \mathbb{R}\}, \tag{12}$$

*where $T(x) = (1 - \sin(\alpha + ix))$. Finally, suppose that $u_n(t)$ is the approximation to $u(t)$ given by the formula*

$$u_n(t) = -\frac{h\lambda}{2\pi i}\sum_{k=-n}^{n} U(\lambda T(kh))T'(kh)e^{\lambda T(kh)t}. \tag{13}$$

*Then the choice of parameters*

$$h = \frac{a(\theta)}{n}, \tag{14}$$

$$\lambda = \frac{2\pi\beta n(1-\theta)}{Ta(\theta)}, \tag{15}$$

$$a(\theta) = \operatorname{arccosh}\left(\frac{2T}{\delta(1-\theta)\sin\alpha}\right) \tag{16}$$

*leads to the uniform estimate on* $\delta \leq t \leq T$,

$$\|u(t) - u_n(t)\| \leq \frac{1}{\sqrt{t}}\phi(\alpha,\beta) \cdot L(\lambda\delta\sin(\alpha-\beta)/2) \cdot e^{-\frac{2\pi\theta\beta n}{a(\theta)}}, \tag{17}$$

*where*

$$\phi(\alpha,\beta) = \frac{2}{\pi}\sqrt{\frac{1+\sin(\alpha+\beta)}{1-\sin(\alpha+\beta)}}(e\sin(\alpha-\beta))^{1/2}, \tag{18}$$

$$L(x) = 1 + |\ln(1 - e^{-x})|. \tag{19}$$

*Proof.* Choosing $s = \frac{1}{2}$, $\mu = \frac{1}{2}$ in the first equation of Remark 2 of [33], we have the estimate

$$\|u(t) - u_n(t)\| \leq$$
$$\frac{\phi(\alpha,\beta)e^{\lambda t}}{2\sqrt{t}}L(\lambda t\sin(\alpha-\beta)/2)\left(\frac{1}{e^{2\pi\beta/h}-1} + \frac{1}{e^{\lambda t\sin\alpha\cosh(nh)/2}}\right). \tag{20}$$

With the choice of parameters given by (14)-(16), it is easy to see that

$$e^{\lambda t} = e^{\frac{2\pi\beta n(1-\theta)t}{Ta(\theta)}} \leq e^{\frac{2\pi\beta n(1-\theta)}{a(\theta)}}, \qquad \delta \leq t \leq T, \tag{21}$$

$$\frac{1}{e^{2\pi\beta}h-1} \approx e^{-2\pi\beta/h} = e^{-\frac{2\pi\beta n}{a(\theta)}}, \tag{22}$$

$$\frac{1}{e^{\lambda t\sin\alpha\cosh(nh)}/2} = e^{-\frac{2\pi\beta nt}{a(\theta)\delta}} \leq e^{-\frac{2\pi\beta n}{a(\theta)}}, \qquad \delta \leq t \leq T, \tag{23}$$

Finally, it is easy to see that $L(x)$ is decreasing in $x$ and thus

$$L(\lambda t\sin(\alpha-\beta)/2) \leq L(\lambda\delta\sin(\alpha-\beta)/2), \qquad \delta \leq t \leq T. \tag{24}$$

Substituting (21)-(24) into (20), we obtain (17). $\qquad\square$

**Remark 1.** The parameters $\alpha$, $\beta$, and $\theta$ are available for optimization. For our problem, i.e., the sum-of-exponentials approximation of the 1D heat kernel, we choose $\alpha = 0.8$, $\beta = 0.7$ in (18). We have also tested various values of $\theta$ in $(0,1)$. Numerical experiments indicate that the number of nodes needed for a prescribed accuracy is relatively insensitive when $\theta$ is in the range $[0.85, 0.95]$.

6

Combining Lemma 1 and Remark 1, we have the following Corollary.

**Corollary 1.** *Suppose that $0 < \epsilon < 0.1$ is the prescribed relative error and that $T \geq 1000\delta > 0$. Then under the conditions of Lemma 1, the following estimate holds*

$$\|u(t) - u_n(t)\| \leq \frac{1}{\sqrt{t}} \cdot \epsilon, \qquad \delta \leq t \leq T, \tag{25}$$

*if the number of exponentials $n$ satisfies the following estimate:*

$$n = O\left(\left(\log\left(\frac{1}{\epsilon}\right) + \log\log\left(\frac{T}{\delta}\right)\right)\log\left(\frac{T}{\delta}\right)\right). \tag{26}$$

*Proof.* We choose the parameters $\alpha$, $\beta$, and $\theta$ as in Remark 1. The factor $\phi(\alpha, \beta)$ in (17) is just a fixed constant independent of $n$, $T$, and $\delta$. For $T \geq 1000\delta > 0$, the parameter $a(\theta)$ defined in (16) satisfies the estimate

$$a(\theta) = O(\log\frac{T}{\delta}). \tag{27}$$

Moreover, the function $L$ defined in (19) is decreasing for $x > 0$, $L(x) \approx |\ln x|$ as $x \to 0^+$, and $L(x) \to 1$ as $x \to +\infty$. Combining this observation with the assumption (26), we observe that the factor $L(\lambda\delta\sin(\alpha - \beta))$ in (17) satifies the estimate

$$L(\lambda\delta\sin(\alpha - \beta)) \leq C\log\left(\frac{T}{\delta}\right). \tag{28}$$

Substituting (27) and (28) into (17), we obtain

$$\|u(t) - u_n(t)\| \leq \frac{C_1}{\sqrt{t}} \cdot \log\left(\frac{T}{\delta}\right) \cdot e^{-C_2 n/\log\left(\frac{T}{\delta}\right)}. \tag{29}$$

It is then easy to see that (25) follows if $n$ satisfies (26). □

**Remark 2.** For most practical cases, the $\log\log\left(\frac{T}{\delta}\right)$ factor is much smaller than the $\log\left(\frac{1}{\epsilon}\right)$ factor. Thus for a fixed precision $\epsilon$, we will simply say that $n = O\left(\log\left(\frac{T}{\delta}\right)\right)$.

**Remark 3.** The hyperbolic contour is chosen in such a way that the horizontal strip $D_\beta = \{z \in \mathbb{C} : |\mathrm{Im}z| \leq \beta\}$ is transformed into a region bounded by the left branches of two hyperbolas defined as in (12), but with $x$ replaced by $x \pm i\beta$. The reason that such contour is chosen is the (well-known) fact that the trapezoidal rule converges exponentially fast for functions holomorphic on a horizontal strip containing the real axis (see, for example, [43, 44]). We have actually used the midpoint rule to eliminate the occurence of a node directly on the real axis. There is almost no difference in terms of accuracy, but this allows us to assume that all nodes lie in the upper half plane in actual computation.

**Remark 4.** It is likely that other contours would yield similar results. Trefethen *et al.* [47] have analyzed this issue with great care and presented a detailed comparison of various contours (hyperbolic, parabolic, and Talbot contours [46]) for inverting sectorial Laplace transforms, though they are mainly concerned with the efficiency of various contours for a fixed time $t$.

We will also need the following lemma, adapted from Theorem 5 in [6], which is concerned with the efficient sum-of-exponentials approximation for the power function $\frac{1}{t^\beta}$.

**Lemma 2.** [Adapted from Theorem 5 in [6].] *For any $\beta \geq \frac{1}{2}$, $1/e \geq \epsilon > 0$, and $T > 3\delta > 0$, there exist a positive integer*

$$N = O\left(\log\left(\frac{1}{\epsilon}\right) \cdot \left(\log\frac{T}{\delta} + \log\frac{1}{\epsilon}\right)\right), \tag{30}$$

*and positive real numbers $\tilde{w}_i$, $\lambda_i$ $(i = 1, \cdots, N)$ such that*

$$\left| \frac{1}{t^\beta} - \sum_{i=1}^{N} \tilde{w}_i e^{-\lambda_i t} \right| \leq \frac{1}{t^\beta} \cdot \epsilon, \qquad \delta \leq t \leq T. \tag{31}$$

*Furthermore, for fixed accuracy $\epsilon$, $N = O\left(\log\frac{T}{\delta}\right)$.*

**Remark 5.** It is pointed out in the caption of Table 1 of [6] that the dependence of the number of terms on accuracy appears to be almost linear in $\log\frac{1}{\epsilon}$ rather than $O\left((\log\frac{1}{\epsilon})^2\right)$, as stated in (30). Indeed, Remark 8 in [25] states that the number of exponentials needed to approximate $\frac{1}{t^{1/2}}$ for a given relative accuracy $\epsilon$ is $O\left(\log\frac{1}{\epsilon}\left(\log\log\frac{1}{\epsilon} + \log\frac{T}{\delta}\right)\right)$. It is straightforward, but tedious, to extend the proof of [25] to show that the number of exponentials to achieve a relative accuracy of $\epsilon$ for $\frac{1}{t^{n/2}}$ when $n = 2, 3, 4$ is of the same order. This is sufficient for the heat kernel in one, two, and three dimensions. While this leads to a formal improvement in estimating the required number of exponentials, the numerical results from the method of [6] are actually more efficient than those obtained via the explicit construction of [25]. Thus, we have left the statement of Lemma 2 as is.

**Remark 6.** In [7], the error of the approximation of $1/x$ by exponential sums is studied in detailed on both finite and infinite intervals. In [8], Braess and Hackbusch extend their analysis to the general power function $1/x^\alpha$, $\alpha > 0$, obtaining sharp error estimates for the absolute error.

## 3 Sum-of-exponentials approximation of the heat kernel

In this section, we first develop a separated sum-of-exponentials approximation for the one-dimensional heat kernel. We then extend the approximation to

arbitrary space dimensions, and to directional derivatives of the heat kernel, such as the kernel of the double layer potential $D(\sigma)$.

The one-dimensional result is summarized by the following theorem.

**Theorem 1.** *Let $G(x,t) = \frac{1}{\sqrt{4\pi t}} e^{-\frac{|x|^2}{4t}}$ denote the one-dimensional heat kernel and let its Laplace transform be denoted by $\hat{G}(x,s) = \int_0^\infty e^{-st} G(x,t) dt$. Then, for $s > 0$ and $x \in \mathbb{R}$,*

$$\hat{G}(x,s) = \frac{1}{2\sqrt{s}} e^{-\sqrt{s}|x|}. \tag{32}$$

*Furthermore, let $0.1 > \epsilon > 0$ be fixed accuracy and $T \geq 1000\delta > 0$ . Then there exists a sum-of-exponentials approximation*

$$G_A(x,t) = \sum_{k=-n}^{n} w_k e^{s_k t} e^{-\sqrt{s_k}|x|} \tag{33}$$

*such that*

$$|G(x,t) - G_A(x,t)| < \frac{1}{\sqrt{t}} \cdot \epsilon \tag{34}$$

*for $x \in \mathbb{R}$ and $t \in [\delta, T]$, with*

$$n = \mathcal{O}\left( \log(\frac{T}{\delta}) \left( \log(\frac{1}{\epsilon}) + \log\log\left(\frac{T}{\delta}\right) \right) \right). \tag{35}$$

*Proof.* The formula (32) is well-known and can be derived from standard Laplace transform tables. The natural extension of $\hat{G}(x,s)$ to the complex $s$-plane has an obvious branch point at $s = 0$, and a branch cut along the negative real axis assuming the restriction $-\pi < s \leq \pi$. Thus, $\hat{G}(x,s)$ is holomorphic on $W = \mathbb{C} \setminus (-\infty, 0]$ and satisfies the estimate

$$\|\hat{G}(x,s)\| \leq \frac{1}{2|s|^{1/2}} \tag{36}$$

for $s \in W$ and all $x \in \mathbb{R}$. As a result, $G(x,t)$ can be represented by the inverse Laplace transform:

$$\begin{aligned}
G(x,t) &= \frac{1}{2\pi i} \int_\Gamma e^{st} \hat{G}(x,s) ds \\
&= \frac{1}{4\pi i} \int_\Gamma \frac{1}{\sqrt{s}} e^{st - \sqrt{s}|x|} ds,
\end{aligned} \tag{37}$$

where $\Gamma$ is a simple contour lying in $W = \mathbb{C} \setminus (-\infty, 0]$, and parametrizable by a regular mapping $S : (-\infty, +\infty) \to \mathbb{C}$ such that

$$\lim_{x \to \pm\infty} \mathrm{Im} S(x) = \pm\infty \qquad \text{and} \qquad \lim_{x \to \pm\infty} \frac{\mathrm{Re}\,(S(x))}{|x|} < 0.$$

9

The last condition implies that

$$\text{Re}(z) \le -b|z|, \qquad \text{as } z \to \infty, z \in \Gamma,$$

for some $b > 0$. This forces the integral (37) to be absolutely convergent. It is easy to see that the integral is independent of the choice of $\Gamma$.

The main result (33) is now a direct consequence of Lemma 1 and Corollary 1 in Section 2 since $\hat{G}$ satisfies the condition (36). In particular, we have

$$G_A(x,t) = \sum_{k=-n}^{n} w_k e^{s_k t} e^{-\sqrt{s_k}|x|}, \tag{38}$$

where

$$s_k = \lambda(1 - \sin(\alpha + ikh)), \tag{39}$$

$$w_k = -\frac{h}{4\pi i \sqrt{s_k}} s_k', \tag{40}$$

with $s_k' = -\lambda i \cos(\alpha + ikh)$, and the parameters $h$, $\lambda$ specified in (14) and (15), respectively. $\qquad\square$

In Table 1, we list the number of exponentials needed to approximate the 1D heat kernel for $x \in \mathbb{R}$ over three different time intervals $[\delta, T]$: $I_1 = [10^{-3}, 1]$, $I_2 = [10^{-3}, 10^3]$, $I_3 = [10^{-5}, 10^4]$, which correspond roughly to $10^3$, $10^6$, and $10^9$ time steps, respectively. The first column lists the maximum error of the approximation computed over a $50 \times 1000$ grid $(x_j, t_k)$ where $x_0 = 0$, $x_j = 2^{-16+j}$ for $j = 1, \cdots, 49$, and the $t_k$ are 1000 samples on $[\delta, T]$ chosen to be equispaced on a logarithmic scale. The node locations are plotted in Fig. 1.

**Table 1: Number of exponentials needed to approximate the 1D heat kernel for $x \in \mathbb{R}$ over different time intervals: $I_1 = [10^{-3}, 1]$, $I_2 = [10^{-3}, 10^3]$, $I_3 = [10^{-5}, 10^4]$.**

| $\epsilon$ | $I_1$ | $I_2$ | $I_3$ |
|---|---|---|---|
| $10^{-3}$ | 15 | 23 | 32 |
| $10^{-6}$ | 31 | 50 | 68 |
| $10^{-9}$ | 47 | 77 | 105 |

**Remark 7.** To obtain Table 1, we set $\alpha = 0.8$, $\beta = 0.7$, $\theta = 0.9$ for $I_1$ and $\theta = 0.95$ for $I_2$ and $I_3$.

**Remark 8.** The coefficients $w_i$ are not positive (but complex) and thus stability is an issue. It is difficult to bound the expression

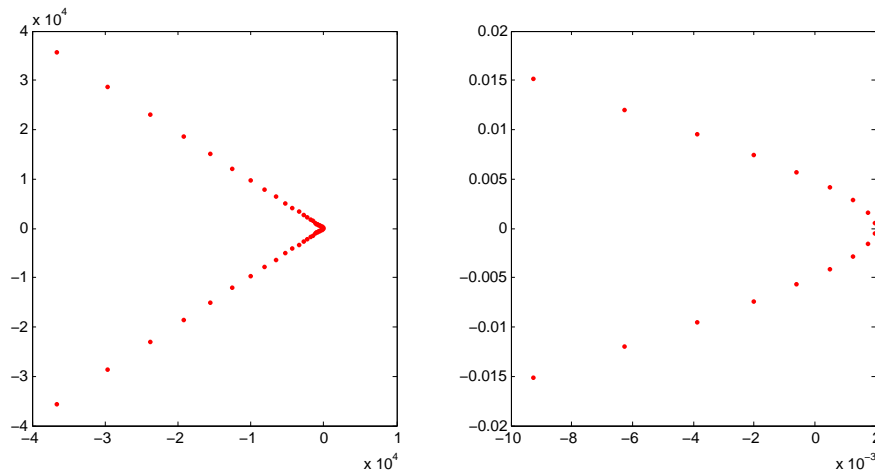$$\frac{\sum |w_i \exp(s_i t)|}{|\sum w_i \exp(s_i t)|}$$

Figure 1: *The location of the exponential nodes $s_k$ ($k = \pm 1, \cdots, \pm n$ for $n = 77$) used in (38) to approximate the 1D heat kernel for $t \in [10^{-3}, 10^3]$ with 9-digit accuracy. The left figure shows all nodes, while the right figure is a close-up of the nodes near the origin. All nodes lie on the left branch of the hyperbola specified in (12).*

analytically for all time. However, we have checked the value of the expression numerically for all cases presented in Table 1, and found that it is roughly 1.08. This suggests that the sum-of-exponentials approximation is, indeed, well-conditioned.

**Remark 9.** If we make a further change of variable $z = \sqrt{s}$ in (37), we obtain

$$G(x,t) = \frac{1}{2\pi i} \int_{\Gamma'} e^{z^2 t - z|x|} dz, \tag{41}$$

where $\Gamma'$ is any contour lying in the sector $\{\frac{\pi}{4} < |\arg z| \leq \frac{\pi}{2}\}$ of the complex plane. In particular, if $\Gamma'$ is chosen to be the imaginary axis, then we essentially recover the Fourier integral representation of the heat kernel (see, for example, [19]).

Finally, it is worth repeating that the number of terms required in the sum-of-exponentials approximation does not depend on the spatial extent of the problem.

## 3.1 Heat kernels in higher dimensions

Suppose now that we are interested in heat flow in $\mathbb{R}^d$, for $d \geq 2$, where the heat kernel is

$$G_d(x,t) = \frac{1}{(4\pi t)^{d/2}} e^{-\frac{|x|^2}{4t}}.$$

11

The following theorem describes an efficient sum-of-exponentials representation.

**Theorem 2.** *For any $0.1 > \epsilon > 0$ and $T \geq 1000\delta > 0$, the heat kernel $G_d(x, t)$ admits the following approximation:*

$$\tilde{G}_d(x, t) = \sum_{j=1}^{N_2} \tilde{w}_j e^{-\lambda_j t} \sum_{k=-N_1}^{N_1} w_k e^{s_k t} e^{-\sqrt{s_k}|x|} \tag{42}$$

*such that*

$$|G_d(x, t) - \tilde{G}_d(x, t)| < \frac{1}{t^{d/2}} \cdot \epsilon \tag{43}$$

*for any $x \in \mathbb{R}^d$, $t \in [\delta, T]$ with $N_1$ specified in (35) and $N_2$ specified in (30).*

*Proof.* We first rewrite the $d$ dimensional heat kernel as a product of two functions:

$$G_d(x, t) = G_1(x, t) \cdot F(t), \tag{44}$$

where

$$G_1(x, t) = \frac{1}{(4\pi t)^{1/2}} e^{-\frac{|x|^2}{4t}}, \qquad F(t) = \frac{1}{(4\pi t)^{(d-1)/2}}. \tag{45}$$

Similarly, we rewrite $\tilde{G}_d$ as follows:

$$\tilde{G}_d(x, t) = S_1(x, t) \cdot S_2(t), \tag{46}$$

where

$$S_1(x, t) = \sum_{k=-N_1}^{N_1} w_k e^{s_k t} e^{-\sqrt{s_k}|x|}, \qquad S_2(t) = \sum_{j=1}^{N_2} \tilde{w}_j e^{-\lambda_j t}. \tag{47}$$

Using the triangle inequality, we have

$$
\begin{aligned}
|G_d(x, t) - \tilde{G}_d(x, t)| &\leq |G_1 \cdot F - G_1 \cdot S_2| + |G_1 \cdot S_2 - S_1 \cdot S_2| \\
&\leq |G_1| \cdot |F - S_2| + (1 + \epsilon)|F| \cdot |G_1 - S_1| \\
&\leq \frac{3}{t^{d/2}} \cdot \epsilon,
\end{aligned}
\tag{48}
$$

and the result follows. $\qquad\square$

## 3.2 The double layer heat potential

Since we often rely on the double layer potential in integral equation methods, it is worth writing down a sum-of-exponentials approximation for this case as well. We denote the kernel of the double layer heat potential by

$$D(x, y; t) = \frac{\partial G(x - y, t)}{\partial n_y} = \frac{(x - y) \cdot n_y}{(4\pi t)^{d/2} 2t} e^{-\frac{|x-y|^2}{4t}}.$$

**Theorem 3.** *Let $0.1 > \epsilon > 0$ be fixed accuracy, $R > 1$ and $T \geq 1000\delta > 0$. Then there exists a sum-of-exponentials approximation*

$$D_A(x, y; t) = \sum_{j=1}^{N_2} \tilde{w}_j e^{-\lambda_j t} \sum_{k=-N_1}^{N_1} w_k e^{s_k t} e^{-\sqrt{s_k}|x-y|}(x-y) \cdot n_y \qquad (49)$$

*such that*

$$|D(x, y; t) - D_A(x, y; t)| < \frac{1}{t^{(d+2)/2}} \cdot \epsilon \qquad (50)$$

*for $|x - y| \leq R$ and $t \in [\delta, T]$. Here $N_1$ and $N_2$ are as follows:*

$$N_1 = \mathcal{O}\left(\log(\frac{T}{\delta})\left(\log(\frac{1}{\epsilon}) + \log\log\left(\frac{T}{\delta}\right) + \log R\right)\right) \qquad (51)$$

*and*

$$N_2 = O\left((\log\left(\frac{1}{\epsilon}\right) + \log R) \cdot \left(\log\frac{T}{\delta} + \log\frac{1}{\epsilon} + \log R\right)\right). \qquad (52)$$

*Proof.* We first introduce $\hat{\epsilon} = \epsilon/R$. Then by Theorem 1, there exist $N_1 = \mathcal{O}\left(\log(\frac{T}{\delta})\log(\frac{1}{\hat{\epsilon}})\right) = \mathcal{O}\left(\log(\frac{T}{\delta})\left(\log(\frac{1}{\epsilon}) + \log\log\left(\frac{T}{\delta}\right) + \log R\right)\right)$, coefficients $w_k$, and nodes $s_k$ $(k = 1, \cdots, N_1)$ such that

$$|G_1(x, t) - \sum_{k=-N_1}^{N_1} w_k e^{s_k t} e^{-\sqrt{s_k}|x|}| < \frac{1}{\sqrt{t}} \cdot \hat{\epsilon}, \qquad (53)$$

for $x \in \mathbb{R}$ and $t \in [\delta, T]$.

Changing $x$ to $x - y$ and multiplying both sides of (53) by $(x - y) \cdot n_y$, we obtain

$$\left|\frac{(x-y) \cdot n_y}{(4\pi t)^{1/2}} e^{-\frac{|x-y|^2}{4t}} - \sum_{k=-N_1}^{N_1} w_k e^{s_k t} e^{-\sqrt{s_k}|x-y|} \cdot ((x-y) \cdot n_y)\right|$$

$$\leq \frac{|(x-y) \cdot n_y|}{(4\pi t)^{1/2}} \cdot \hat{\epsilon}$$

$$\leq \frac{R}{(4\pi t)^{1/2}} \cdot \frac{\epsilon}{R} \qquad (54)$$

$$\leq \frac{1}{(4\pi t)^{1/2}} \cdot \epsilon$$

for all $|x - y| \leq R$ and $t \in [\delta, T]$.

Similarly, by Lemma 2, we have

$$\left|\frac{1}{t^{(d+1)/2}} - \sum_{i=1}^{N_2} \tilde{w}_i e^{-\lambda_i t}\right| \leq \frac{1}{t^{(d+1)/2}} \cdot \epsilon/R, \qquad \delta \leq t \leq T, \qquad (55)$$

where $N_2$ is given by (52).

The result is then obtained by an argument almost identical to that in the proof of Theorem 2. $\qquad \square$

**Remark 10.** As discussed in Remark 5, more involved analysis could replace the order estimate $O((\log \frac{1}{\epsilon} + \log R)^2)$ for $N_2$ in (52) with $O(\log \frac{1}{\epsilon} + \log R)$.

**Remark 11.** It is worth noting that Theorems 1–3 provide what are, in essence, relative error estimates. Our numerical experiments also indicate that the $\log R$ dependence in $N_1$ and $N_2$ and the restriction on $x - y$ are somewhat artificial since $D(x, y; t)$ and $D_A(x, y; t)$ are exponentially small for large $(x - y)$.

## 4 Applications

We return now to a consideration of the exterior Dirichlet problem governed by the heat equation in eqs. (1) and (2). We let $\delta = (k - 1)\Delta t$ in order to obtain a $k$th order scheme and consider the calculation of $D_L$ and $D_H$ separately. To simplify the notation, we fix the relative accuracy $\epsilon$, the computational domain size $R$, and suppress the dependence of the complexity on $\epsilon$ and $R$ in the following discussion.

### 4.1 Evaluation of the local part $D_L$

The discretization of the local part of the double layer potential $D_L$ is discussed in [31] for both stationary and moving boundaries. We limit our attention here to the case of a stationary boundary, $\Gamma(t) = \Gamma(0)$, for the sake of simplicity. The basic idea is to expand the density $\sigma(y, t)$ on $[t - \delta, t]$ for each $y$ in the form

$$\sigma(y, \tau) = \sigma_0(y) + (t - \tau)\sigma_1(y) + \cdots + \frac{(t - \tau)^{k-1}}{(k - 1)!}\sigma_{k-1}(y) + O((t - \tau)^k).$$

The functions $\sigma_0(y), \ldots, \sigma_{k-1}(y)$ are obtained from the function values $\sigma(y, t - j\Delta t)$ for $j = 0, \cdots, k - 1$.

Substituting the above expression into (8) and changing the order of integration in time and space, we obtain

$$D_L(\sigma)(x, t, \delta) = \left[ \int_\Gamma D_{L,0}(x, y)\sigma_0(y)\, ds_y + \int_\Gamma D_{L,1}(x, y)\sigma_1(y)\, ds_y + \ldots \right.$$

$$\tag{56}$$

$$\left. + \frac{1}{(k - 1)!} \int_\Gamma D_{L,k-1}(x, y)\sigma_{k-1}(y)\, ds_y \right] + O((t - \tau)^{k+1/2}).$$

where $D_{L,k}(x, y)$ is given by

$$D_{L,k}(x, y) = \int_{t-\delta}^t \frac{\partial}{\partial n_y} G_d(x - y, t - \tau)(t - \tau)^{k-2}\, d\tau. \tag{57}$$

For an analgous treatment of unsteady Stokes potentials, see [27].

**Remark 12.** The above procedure provides a robust, high-order marching scheme that is insensitive to the complexity of the geometry. Simpler time-marching schemes are subject to *geometrically induced stiffness*, discussed at some length in [27, 31].

The kernels $D_{L,k}$ can be computed in closed form in terms of the exponential integral function $\text{Ei}(1, x)$ in two dimensions and the error function $\text{erf}(x)$ in three dimensions. Each of these kernels is singular (or weakly singular), but smooth away from the diagonal ($x = y$). The discretization of the spatial integrals, therefore, requires techniques much like those needed for elliptic layer potentials. We refer the reader to [1] and [28] for a discussion of high order accurate rules.

When computing $D_{L,k}$ at each boundary point, we would also like to avoid the $O(N_S^2)$ work that would be required by naive evaluation of the integral. A large number of fast algorithms are now available to reduce the cost of this step to $O(N_S)$ or $O(N_S \log N_S)$. These include fast multipole methods, kernel-independent fast multipole methods [50], HSS and H-matrix methods [12, 21], and HBS or recursive skeletonization methods [23, 17]. We propose to use the approach developed in [23]. That is, each of the operators $D_{L,j}(x_m, y_n)$ ($j = 1, \cdots, k - 1$) will be compressed once, with subsequent applications of the operator computed in near optimal complexity time with smaller constant prefactors than analytically-based fast multipole methods. It is also possible, of course, to store a compressed version of the full operator $D_L$ or $(-\frac{1}{2}I + D_L^*)^{-1}$. While the storage costs are large, they scale nearly linearly with $N_S$. This is ideal for long-time simulation in stationary domains, where the same linear system is solved at each time step with a different right-hand side.

## 4.2   Evaluation of the history part $D_H$

For the history part, approximating the kernel by $D_A(x, y; t-\tau)$ and substituting (49) into (7), we obtain

$$
\begin{aligned}
D_H(\sigma)(x,t) \approx \int_0^{t-\delta} \int_\Gamma \sum_{j=1}^{N_2} \tilde{w}_j e^{-\lambda_j(t-\tau)} \\
\sum_{k=-N_1}^{N_1} w_k e^{s_k(t-\tau)} e^{-\sqrt{s_k}|x-y|} [(x-y) \cdot n_y] \sigma(y, \tau) ds_y d\tau \\
= \sum_{j=1}^{N_2} \tilde{w}_j \sum_{k=-N_1}^{N_1} w_k H_{j,k}(x,t),
\end{aligned} \tag{58}
$$

where each history mode $H_{j,k}$ is given by the formula

$$
H_{j,k}(x,t) = \int_0^{t-\delta} e^{(-\lambda_j + s_k)(t-\tau)} V_k(x, \tau) d\tau, \tag{59}
$$

with $V_k$ given by the formula

$$
V_k(x, \tau) = \int_\Gamma e^{-\sqrt{s_k}|x-y|} [(x-y) \cdot n_y] \sigma(y, \tau) ds_y. \tag{60}
$$

Here, we have interchanged the order of summation and integration.

For each fixed $\tau$, $V_k(x,\tau)$ can be discretized using the trapezoidal rule and the resulting summation can again be computed using the fast algorithms in [23] for all $x \in \Gamma$. The computational cost for this step is $\mathcal{O}(N_S \log N_S)$ for each $k$. Once the $V_k$ have been evaluated, each history mode $H_{j,k}$ can be computed recursively, as in [19, 27]:

$$H_{j,k}(x,t+\Delta t) = e^{(-\lambda_j+s_k)\Delta t}H_{j,k}(x,t) + \int_{t-\delta}^{t+\Delta t-\delta} e^{(-\lambda_j+s_k)(t+\Delta t-\tau)}V_k(x,\tau)d\tau.$$

(Equivalently, each history mode $H_{j,k}$ can be seen to satisfy a simple linear ODE.) The point is that each history mode can be computed in $\mathcal{O}(1)$ operations at each time step for each $x$. Since both $N_1$ and $N_2$ are $\mathcal{O}(\log(T/\delta)) = \mathcal{O}(N_T)$ with $N_T$ the total number of time steps, the net computational cost for the evaluation of the history part at each time step is $\mathcal{O}(N_S \log N_S \log N_T + N_S \log^2 N_T)$, with storage requirements of the order $\mathcal{O}(N_S \log^2 N_T)$. The computational cost for the entire simulation is

$$\mathcal{O}(N_S N_T \log N_S \log N_T + N_S N_T \log^2 N_T).$$

The algorithm of the present paper is embarrassingly parallel in that the computation of each history mode is independent. Furthermore, the hierarchical fast algorithms used for each $V_k(x,\tau)$ are themselves amenable to parallelization, and there is already a substantial body of research and software devoted to that task for large-scale problems in three dimensions.
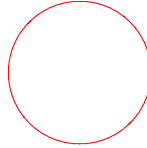
# 5 Numerical examples

In this section, we illustrate the accuracy and stability of the sum-of-exponential approximations for the heat kernels. More precisely, we have implemented the algorithm outlined in the previous section to solve the exterior Dirichlet problem governed by the heat equation in two dimensions. The spatial integral in the local parts is discretized using the 16th order hybrid Gauss-trapezoidal rule of [1], while the spatial integral in the history part is discretized using the trapezoidal rule. We have implemented 2nd, 3rd, and 4th order schemes in time (defined by the number of terms taken in the local Taylor expansion of $\sigma$ in section 4.1), with numerical experiments carried out using the fourth order version. We consider four simple boundary curves: a circle, an ellipse with aspect ratio 2:1, a crescent, and a smooth hexagram, shown in Figures 1–4, respectively. The final time is set to $T = 1$ and the boundary curves are roughly of size $R = 5$. We generate boundary data by placing heat sources *inside* the boundary curve and test the accuracy of our numerical solution by comparing it with the analytical solution at 20 target points outside the boundary curves. We use 350 spatial discretization points for the circle, 256 points for the ellipse, 512 points for the crescent, and 350 points for the hexagram. Since our spatial integration rules are very high order and the geometry is well-resolved, the accuracy is dominated by the discretization error in time.

In each of the tables below, $\Delta t$ is the time step, $N_T$ is the total number of time steps, $K$ is the condition number of the linear system that needs to be solved at each time step, $E$ is the relative $L^2$ error of the numerical solution at the final time, and $r$ is the ratio of relative $L^2$ errors for successive time step refinements: $r(j) = E(j-1)/E(j)$.

**Remark 13.** Since our examples are intended to demonstrate the accuracy and stability of the sum-of-exponential approximations for the heat kernels, we have limited our attention to modest size problems. With larger-scale boundary discretizations, fast solvers will be used to invert the linear systems at each time step and to speed up the computation of the spatial integrals in the history part. We are currently building such codes, including parallelization.

| $\Delta t$ | $N_T$ | $K$ | $E$ | $r$ |
|---|---|---|---|---|
| 1.00e-1 | 10 | 1.02 | 4.33e-5 | |
| 5.00e-2 | 20 | 1.01 | 3.00e-6 | 14.4 |
| 2.50e-2 | 40 | 1.01 | 2.01e-7 | 14.9 |
| 1.25e-2 | 80 | 1.01 | 7.57e-9 | 26.5 |
| 6.25e-3 | 160 | 1.00 | 3.81e-10 | 19.9 |

Figure 2: Numerical results for the circle. $N_T$ is the total number of time steps, $K$ is the condition number of the linear system to be solved at each time step, $E$ is the relative error at the final time in $L^2$, and $r$ is the ratio of relative $L^2$ errors for successive time step refinements: $r(j) = E(j-1)/E(j)$.
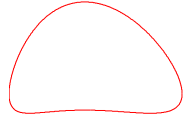
| $\Delta t$ | $N_T$ | $K$ | $E$ | $r$ |
|---|---|---|---|---|
| 1.00e-1 | 10 | 1.07 | 1.85e-4 | |
| 5.00e-2 | 20 | 1.05 | 1.55e-5 | 11.9 |
| 2.50e-2 | 40 | 1.04 | 1.11e-6 | 13.9 |
| 1.25e-2 | 80 | 1.03 | 1.84e-8 | 60.3 |
| 6.25e-3 | 160 | 1.02 | 6.76e-10 | 27.3 |

Figure 3: Numerical results for a 2:1 ellipse. See text or Fig. 2 for explanation.

Several observations concerning our results are in order. First, note that there is no stability issue for large time steps (as expected). Second, the linear systems which need to be solved at each time step are extremely well-conditioned, since the compact operator in the Volterra integral equation has small norm. Third, the convergence rates are roughly consistent with fourth order accuracy (slightly better because of the smoothing behavior of the heat equation).

Finally, in order for the reader to be able to easily implement the scheme, we list the sum-of-exponential approximations for the power function $\frac{1}{t^{3/2}}$ and the 1D heat kernel in Tables 2 and 3, respectively.

17

| $\Delta t$ | $N_T$ | $K$ | $E$ | $r$ |
|---|---|---|---|---|
| 1.00e-1 | 10 | 1.15 | 8.76e-5 | |
| 5.00e-2 | 20 | 1.11 | 3.13e-6 | 28.0 |
| 2.50e-2 | 40 | 1.08 | 1.89e-7 | 16.5 |
| 1.25e-2 | 80 | 1.06 | 3.16e-9 | 59.8 |
| 6.25e-3 | 160 | 1.04 | 1.28e-10 | 24.6 |

Figure 4: Numerical results for a smooth crescent. See text or Fig. 2 for explanation.
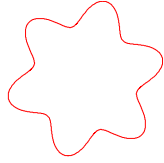


| $\Delta t$ | $N_T$ | $K$ | $E$ | $r$ |
|---|---|---|---|---|
| 1.00e-1 | 10 | 1.03 | 6.05e-5 | |
| 5.00e-2 | 20 | 1.02 | 3.06e-6 | 19.8 |
| 2.50e-2 | 40 | 1.02 | 1.94e-7 | 15.7 |
| 1.25e-2 | 80 | 1.01 | 7.80e-9 | 24.5 |
| 6.25e-3 | 160 | 1.01 | 2.80e-10 | 27.8 |

Figure 5: Numerical results for a smooth hexagram. See text or Fig. 2 for explanation.

Table 2: Sum-of-exponential approximation for the power function $\frac{1}{t^{3/2}} \approx \sum_{k=1}^{N} w_k e^{s_k t}$. Here $N = 22$. The relative error is $10^{-9}$ for $t \in [10^{-3}, 1]$. The first column lists the values of $s_k$ and the second column lists the values of $w_k$.

| $s_k$ | $w_k$ |
|---|---|
| -7.2906159549928551D-001 | 1.4185610815528382D+000 |
| -3.0048118783719833D+000 | 6.1168393596966855D+000 |
| -7.1264765899586058D+000 | 1.5711472927135111D+001 |
| -1.3711947176886415D+001 | 3.4005632951162106D+001 |
| -2.3888158541731844D+001 | 6.9073954353680932D+001 |
| -3.9552395196025927D+001 | 1.3693587825572760D+002 |
| -6.3705812577837150D+001 | 2.6803903557553036D+002 |
| -1.0092380540293159D+002 | 5.1918775664556608D+002 |
| -1.5806801843263241D+002 | 9.9539106627427793D+002 |
| -2.4535153453758187D+002 | 1.8891680379043360D+003 |
| -3.7789560121839855D+002 | 3.5504717885763807D+003 |
| -5.7797736857567725D+002 | 6.6101535364473611D+003 |
| -8.7825970527795960D+002 | 1.2196709015044245D+004 |
| -1.3264302774624159D+003 | 2.2315687874782194D+004 |
| -1.9919031777954062D+003 | 4.0515943857625483D+004 |
| -2.9756729573498451D+003 | 7.3077757126301352D+004 |
| -4.4253961362173968D+003 | 1.3121449467706907D+005 |
| -6.5602925574528726D+003 | 2.3547202449444451D+005 |
| -9.7174072351500563D+003 | 4.2563843229579012D+005 |
| -1.4450262425240786D+004 | 7.8639206472664094D+005 |
| -2.1750443538417538D+004 | 1.5127774335123657D+006 |
| -3.3020803685636522D+004 | 2.6486986425576657D+006 |

Table 3: Sum-of-exponential approximation for the 1D heat kernel $G_1 = e^{-x^2/4t}/\sqrt{4\pi t}$. $G_1 \approx \sum_{k=-N_1}^{N_1} w_k e^{s_k t} e^{-\sqrt{s_k} x}$. Here $N_1 = 47$ and only the exponentials in the lower half of the complex plane are listed. The relative error is $10^{-9}$ for $t \in [10^{-3}, 1]$. The first column lists the values of $s_k$ and the second column lists the values of $w_k$.

| $s_k$ | $w_k$ |
| --- | --- |
| +5.2543538566883130D-001 -1.5355921434143971D-001i | 3.3406450069243053D-002 + 7.8694879334856565D-004i |
| +4.5124072851051300D-001 -4.6901795847816991D-001i | 3.3585524697168449D-002 + 2.3714958079918535D-003i |
| +2.9882165376338349D-001 -8.0995063945421741D-001i | 3.4768791677853524D-002 + 3.9881352204446229D-003i |
| +5.9899770775166200D-002 -1.1948744535190035D+000i | 3.6149569249415578D-002 + 5.6587442927134319D-003i |
| -2.7850156846250274D-001 -1.6446959027588257D+000i | 3.8019542860491549D-002 + 7.4059306342027370D-003i |
| -7.3476207454759612D-001 -2.1838462972755117D+000i | 4.0404018032102237D-002 + 9.2533381404359474D-003i |
| -1.3336627843342230D+000 -2.8416087014987785D+000i | 4.3335262806011098D-002 + 1.1225966955375540D-002i |
| -2.1077320020767232D+000 -3.6537083955326728D+000i | 4.6852944413778977D-002 + 1.3350511787250059D-002i |
| -3.0990120206246341D+000 -4.6642532348208814D+000i | 5.1004666075762921D-002 + 1.5655723156165313D-002i |
| -4.3613425792163030D+000 -5.9281292955658031D+000i | 5.5846611194320855D-002 + 1.8172796462103385D-002i |
| -5.9632850801149733D+000 -7.5139819214310553D+000i | 6.1444303658802629D-002 + 2.0935794138393353D-002i |
| -7.9918463880908517D+000 -9.5079440821622647D+000i | 6.7873494551196165D-002 + 2.3982106603468702D-002i |
| -1.0557204464776218D+001 -1.2018314543775274D+001i | 7.5221187251822183D-002 + 2.7352958248766927D-002i |
| -1.3798692502929331D+001 -1.5181439937409575D+001i | 8.3586841817376690D-002 + 3.1093965310080390D-002i |
| -1.7892366578989638D+001 -1.9169120201715121D+001i | 9.3083585564254306D-002 + 3.5255753171782450D-002i |
| -2.3060567848491313D+001 -2.4197939613161662D+001i | 1.0384001506633338D-001 + 3.9894641457634002D-002i |
| -2.9583998639207351D+001 -3.0541030203791603D+001i | 1.1600166529906714D-001 + 4.5073406179197625D-002i |
| -3.7816968335105827D+001 -3.8542906477049684D+001i | 1.2973311446494412D-001 + 5.0862129255676444D-002i |
| -4.8206637106159420D+001 -4.8638177148812161D+001i | 1.4522018415709023D-001 + 5.7339146901350516D-002i |
| -6.1317302675453163D+001 -6.1375150182749685D+001i | 1.6267245400022495D-001 + 6.4592109714717016D-002i |
| -7.7861049219288773D+001 -7.7445613273673700D+001i | 1.8232609779849215D-001 + 7.2719168815048321D-002i |
| -9.8736423044743205D+001 -9.7722407114526959D+001i | 2.0444707957048894D-001 + 8.1830304077826238D-002i |
| -1.2507723565031891D+002 -1.2330683231921709D+002i | 2.2933475272201531D-001 + 9.2048812443472808D-002i |
| -1.5831414482743193D+002 -1.5558846474502963D+002i | 2.5732591106254793D-001 + 1.0351297643999625D-001i |
| -2.0025235847869459D+002 -1.9632062801341692D+002i | 2.8879934648604044D-001 + 1.1637793549892739D-001i |
| -2.5316968150772374D+002 -2.4771562239065099D+002i | 3.2418097499311860D-001 + 1.3081778538823258D-001i |
| -3.1994023103558078D+002 -3.1256488222792592D+002i | 3.6394960042284941D-001 + 1.4702793417289575D-001i |
| -4.0419053933177224D+002 -3.9439058811408586D+002i | 4.0864339389209720D-001 + 1.6522774658533385D-001i |
| -5.1049652293304160D+002 -4.9763696830499521D+002i | 4.5886717662584403D-001 + 1.8566351259073638D-001i |
| -6.4463201600277023D+002 -6.2791167965116256D+002i | 5.1530060473377282D-001 + 2.0861178031960287D-001i |
| -8.1388236661047688D+002 -7.9229037823057672D+002i | 5.7870736669405309D-001 + 2.3438309847056926D-001i |
| -1.0274401283961181D+003 -9.9970102193834418D+002i | 6.4994551800979161D-001 + 2.6332621882780033D-001i |
| -1.2969043389592882D+003 -1.2614087777944171D+003i | 7.2997909289244700D-001 + 2.9583281576374076D-001i |
| -1.6369105024555524D+003 -1.5916278709100643D+003i | 8.1989115010796476D-001 + 3.3234278659416305D-001i |
| -2.0659254928655710D+003 -2.0082936066805410D+003i | 9.2089842952925771D-001 + 3.7335020451285178D-001i |
| -2.6072505517969930D+003 -2.5340364973160094D+003i | 1.0343678177356390D+000 + 4.1941000466434852D-001i |
| -3.2902868569904354D+003 -3.1974114007865637D+003i | 1.1618348454808407D+000 + 4.7114549383439813D-001i |
| -4.1521323987955984D+003 -4.0344484308358847D+003i | 1.3050244673476217D+000 + 5.2925678538340226D-001i |
| -5.2395968963294799D+003 -5.0906098731829061D+003i | 1.4658744047907917D+000 + 5.9453027356908161D-001i |
| -6.6117441901645352D+003 -6.4232593945873459D+003i | 1.6465613684596623D+000 + 6.6784927547013706D-001i |
| -8.3431001974123810D+003 -8.1047776557969619D+003i | 1.8495305146549577D+000 + 7.5020598452333265D-001i |
| -1.0527700663992231D+004 -1.0226493547754852D+004i | 2.0775285345412993D+000 + 8.4271489743589800D-001i |
| -1.3284198561072539D+004 -1.2903644569677639D+004i | 2.3336408238968738D+000 + 9.4662789617368170D-001i |
| -1.6762308525499571D+004 -1.6281635763758291D+004i | 2.6213332364019597D+000 + 1.0633511891228977D+000i |
| -2.1150938363365654D+004 -2.0543937150208803D+004i | 2.9444989854949983D+000 + 1.1944643406826623D+000i |
| -2.6688449265921696D+004 -2.5922048598801452D+004i | 3.3075113294981566D+000 + 1.3417416460873389D+000i |
| -3.3675602004538763D+004 -3.2708073362471001D+004i | 3.7152827529767691D+000 + 1.5071761457643933D+000i |

# 6    Conclusions

We have developed an efficient separated sum-of-exponentials approximation for the heat kernel in any dimension. The number of exponentials needed is $\mathcal{O}(\log^2(\frac{T}{\delta}))$ to obtain an approximation that is valid for $t \in [\delta, T]$ and $x \in \mathbb{R}^d$ for any prescribed precision $\epsilon$, but only $\mathcal{O}(\log(\frac{T}{\delta}))$ of these modes involve the spatial variables. Such approximations can be combined with the local quadratures of [31] and the fast algorithms of [18, 19, 23] to create efficient, accurate and robust methods for the solution of boundary value problems governed by the heat equation in complex geometry.

We have assumed here that the time step $\Delta t$ is fixed throughout the simulation, but note that in many applications, adaptive time-stepping will be needed. We are currently developing heat solvers in both two and three dimensions that make use of the sum-of-exponentials representation, permit adaptive time-steps, and incorporate fast algorithms for the spatial integrals. We will report on their performance at a later date.

# References

[1] B. K. Alpert, *Hybrid Gauss-trapezoidal quadrature rules.* SIAM J. Sci. Comput., **20** (1999), 1551–1584.

[2] B. Alpert, L. Greengard, and T. Hagstrom, *Rapid evaluation of nonreflecting boundary kernels for time-domain wave propagation.* SIAM J. Numer. Anal. **37** (2000), no. 4, 1138–1164.

[3] B. Alpert, L. Greengard, and T. Hagstrom, *Nonreflecting boundary conditions for the time-dependent wave equation.* J. Comput. Phys. **180** (2002), no. 1, 270–296.

[4] G. Beylkin and L. Monzón, *On Generalized Gaussian Quadrature for Exponentials and their Applications.* Appl. Comput. Harmon. Anal. **12** (2002), 332-373.

[5] G. Beylkin and L. Monzón, *On approximation of functions by exponential sums.* Appl. Comput. Harmon. Anal. **19** (2005), 17-48.

[6] G. Beylkin and L. Monzón, *Approximation by exponential sums revisited.* Appl. Comput. Harmon. Anal. **28** (2010), 131-140.

[7] D. Braess and W. Hackbusch, *Approximation of $1/x$ by exponential sums in $[1, \infty)$.* IMA J. Numer. Anal. **25** (2005), no. 4, 685–697.

[8] D. Braess and W. Hackbusch, *On the efficient computation of high-dimensional integrals and the approximation by exponential sums.* Multiscale, nonlinear and adaptive approximation, 39–74, Springer, Berlin, 2009.

[9] K. Brattkus and D. I. Meiron, *Numerical simulations of unsteady crystal growth*, SIAM J. Appl. Math. **52**, (1992), 1303–1320.

[10] Brebbia, C. A. (ed.), *Topics in Boundary Element Research*, Vol. 1, Springer-Verlag, Berlin (1981).

[11] J. Bremer, Z. Gimbutas, and V. Rokhlin, *A nonlinear optimization procedure for generalized Gaussian quadratures.* SIAM J. Sci. Comput. **32** (2010), no. 4, 1761–1788.

[12] S. Chandrasekaran, P. Dewilde, M. Gu, W. Lyons, and T. Pals, *A fast solver for HSS representations via sparse matrices*, SIAM J. Matrix Anal. Appl. **29** (2006), 67–81.

[13] R. Chapko and R. Kress, *Rothe's method for the heat equation and boundary integral equations.* J. Integral Equations Appl. **9** (1997), no. 1, 47–69.

[14] H. Cheng, L. Greengard, and V. Rokhlin, *A fast adaptive multipole algorithm in three dimensions.* J. Comput. Phys. **155** (1999), no. 2, 468–498.

[15] M. Costabel, *Time-dependent problems with the boundary integral equation method.* Chapter 25, Encyclopedia of Computational Mechanics, (E. Stein, R. De Borst, T.J.R. Hughes, eds), John Wiley, 2004.

[16] A. Friedman, *Partial Differential Equations of Parabolic Type*, Prentice-Hall, Englewood Cliffs, New Jersey, 1964.

[17] A. Gillman, P. Young, and P. G. Martinsson, *A direct solver with O(N) complexity for integral equations on one-dimensional domains*, Front. Math. China, **7** (2012), 217–247.

[18] L. Greengard and P. Lin, *Spectral approximation of the free-space heat kernel.* Appl. Comput. Harmon. Anal., **9** (2000), 83–97.

[19] L. Greengard and J. Strain, *A fast algorithm for the evaluation of heat potentials.* Comm. Pure Appl. Math., **43** (1990), 949–963.

[20] R. B. Guenther and J. W. Lee, *Partial Differential Equations of Mathematical Physics and Integral Equations.* Prentice-Hall, Englewood Cliffs, New Jersey, 1988.

[21] W. Hackbusch and S. Börm, *Data-sparse approximation by adaptive H2-matrices*, Computing **69** (2002), no. 1, 1–35.

[22] T. Hagstrom, *Radiation boundary conditions for the numerical simulation of waves*, Acta Numerica, **8** (1999), 47–106.

[23] K. L. Ho and L. Greengard, *A fast direct solver for structured linear systems by recursive skeletonization.* SIAM J. Sci. Comput. **34** (2012), no. 5, A2507–A2532.

[24] M. T. Ibanez and H. Power, *An efficient direct BEM numerical scheme for phase change problems using Fourier series.* Comput. Methods Appl. Mech. Engrg. **191** (2002), 2371–2402.

[25] S. Jiang and L. Greengard, *Fast evaluation of nonreflecting boundary conditions for the Schrödinger equation in one dimension.* Comput. Math. Appl. **47** (2004), no. 6-7, 955–966.

[26] S. Jiang and L. Greengard, *Efficient representation of nonreflecting boundary conditions for the time-dependent Schrödinger equation in two dimensions.* Comm. Pure Appl. Math. **61** (2008), no. 2, 261–288.

[27] S. Jiang, S. Veerapaneni, and L. Greengard, *Integral equation methods for unsteady Stokes flow in two dimensions.* SIAM J. Sci. Comput. **34** (2012), no. 4, A2197-A2219.

[28] A. Kloeckner, A. Barnett, L. Greengard, and M. ONeil, *Quadrature by Expansion: A New Method for the Evaluation of Layer Potentials.* arXiv:1207.4461, 2012.

[29] R. Kress, *Linear integral equations.* Second Edition, Springer, 1999.

[30] J. R. Li, and L. Greengard, *On the numerical solution of the heat equation. I. Fast solvers in free space.* J. Comput. Phys. **226** (2007), no. 2, 1891–1901.

[31] J. Li and L. Greengard, *High order accurate methods for the evaluation of layer heat potentials.* SIAM J. Sci. Comput., **31** (2009), 3847–3860.

[32] M. López-Fernández and C. Palencia, *On the numerical inversion of the Laplace transform of certain holomorphic mappings.* Applied Numer. Math. **51** (2004), 289-303.

[33] M. López-Fernández, C. Palencia, and A. Schädle, *A spectral order method for inverting sectorial Laplace transforms.* SIAM J. Numer. Anal. **44** (2006), no. 3, 1332-1350.

[34] M. López-Fernández, C. Lubich, and A. Schädle, *Adaptive, fast, and oblivious convolution in evolution equations with memory.* SIAM J. Sci. Comput. **30** (2008), no. 2, 1015-1037.

[35] C. Lubich and A. Schädle, *Fast convolution for nonreflecting boundary conditions.* SIAM J. Sci. Comput. **24** (2002), 161–182.

[36] Morino, L. and Piva, R. (eds.), *Boundary Integral Methods: Theory and Applications.* Springer-Verlag, Berlin, 1990.

[37] J. Ma, V. Rokhlin, and S. Wandzura, *Generalized Gaussian quadrature rules for systems of arbitrary functions.* SIAM J. Numer. Anal. **33** (1996), no. 3, 971–996.

[38] E. A. McIntyre, *Boundary integral solutions of the heat equation.* Math. Comp. **46** (1986), no. 173, 71–79, S1–S14.

[39] P. J. Noon, *The Single Layer Heat Potential and Galerkin Boundary Element Methods for the Heat Equation.* Ph.D. Thesis, University of Maryland, 1988.

[40] W. Pogorzelski, *Integral Equations and Their Applications.* Pergamon Press, Oxford, 1966.

[41] A. Schädle, M. López-Fernández, and C. Lubich, *Fast and oblivious convolution quadrature.* SIAM J. Sci. Comput. **28** (2006), no. 2, 421-438.

[42] J. A. Sethian and Strain, J., *Crystal Growth and Dendritic Solidification.* J. Comput. Phys. **98**, (1992), 231–253.

[43] F. Stenger, *Approximation via Whitaker's Cardinal Functions.* J. Approx. Theory **17** (1976), 222-240.

[44] F. Stenger, *Numerical methods based on Whitaker Cardinal, or sinc Functions.* SIAM Rev. **23** (1981), 165-224.

[45] J. Tausch, *A fast method for solving the heat equation by layer potentials.* J. Comput. Phys. **224** (2007), no. 2, 956–969.

[46] A. Talbot, *The accurate numerical inversion of Laplace transforms.* J. Inst. Math. Appl. **23** (1979), 97-120.

[47] L. N. Trefethen, J. A. C. Weideman, and T. Schmelzer, *Talbot quadratures and rational approximations.* BIT Numer. Math. **46** (2006), 653-670.

[48] K. Xu and S. Jiang, *A Bootstrap Method for Sum-of-Poles Approximations.* J. Sci. Comput. **55** (2013), 16–39.

[49] N. Yarvin and V. Rokhlin, *An improved fast multipole algorithm for potential fields on the line.* SIAM J. Numer. Anal. **36** (1999), no. 2, 629–666.

[50] L. Ying, G. Biros, and D. Zorin, *A kernel-independent adaptive fast multipole algorithm in two and three dimensions.* J. Comput. Phys. **196** (2004), 591–626.